2007-01-2367

Incorporation of Non-Linear and Quasi-Linear Hydraulic Mount Formulations into a Vehicle Model

Song He and Rajendra Singh
Acoustics and Dynamics Laboratory
The Ohio State University

ABSTRACT

This paper comparatively evaluates measurement-based quasi-linear and true non-linear (mechanical and fluid type) models of hydraulic engine mounts and examines their dynamic effects within the context of a simplified half-vehicle system. A non-linear approximate model is also developed to provide improved insight into the decoupling effects. The proposed model is validated by comparing predictions with those from a "true" non-linear fluid model. When embedded into the vehicle system, hydraulic mount efficiently provides high amplitude-sensitive damping and tunes the engine bounce mode. Proposed model concepts could be effectively utilized to examine linear and non-linear vehicle responses in both time and frequency domains.

INTRODUCTION

Over the past two decades, significant research [1-11] has been conducted on the dynamics of non-linear hydraulic engine mounts. Much of the literature [4-9] focuses on its frequency- and excitation amplitude-sensitive properties on a device level, which is necessary but not sufficient from the system viewpoint. This paper aims to fill in this void by incorporating linear, quasi-linear or non-linear mount models into a simplified, yet reasonable, half-vehicle model. This will permit a comparative evaluation of the competing modeling methods in the context of vehicle dynamics. It is of course assumed that the mount properties as measured by the elastomer test machines can be directly "imported" into vehicle models even though there are key differences between the elastomer test method and in-situ vehicle mounting system. In fact, many practitioners use ad hoc methods to bring in measured data (or parameters) in a vehicle model. Accordingly, the following objectives are established: First, propose a simplified half-vehicle model that would incorporate competing mount models (based on elastomer test data). Modal study of the vehicle system, based on the quasi-linear model, will help to answer the key question that certain vehicle modes could be effectively tuned due to a coupling between hydraulic mount and other vehicle components. Second, develop a non-linear approximate model for the free decoupler type hydraulic mount to provide improved insight into the decoupling effects. The switching mechanism will be described in terms of a clearance type non-linearity. Third, estimate effective parameters via the approximate method for reduced modeling efforts. The proposed model will then be validated by comparing predictions with a "true" fluid type model (based on time domain solutions [5]). Finally, the "true" non-linear fluid model will be utilized to examine non-linear dynamic vehicle responses such as the super-harmonics.

INCORORATION OF HYDRAULIC MOUNT FORMULATION(S) INTO HALF-VEHICLE MODEL

Table 1 Comparison of mount sub-system models

Model Type	Linear	Quasi-Linear	"True" Non-Linear (Fluid)	Non-Linear (Approximate method)
Mount (Fig.)	Rubber 1(b)	Hydraulic 1(c)	Hydraulic 1(d)	Hydraulic (1e)
Analysis Domain	Time & Modal	Time & Modal	Time & Freq. (FFT)	Time & Freq. (FFT)
Modeling Efforts Needed	Minimal	Minimal	High	Moderate
DOF of Fig. 1(a)	6 DOF	6+1 DOF	6+2 DOF	6+2 DOF

Fig. 1(a) shows a simplified 6 DOF half-vehicle model with displacements only in the vertical direction x_i (i = 1,…,6). Lumped masses m_1 to m_6 correspond to the inertia elements of the engine, front vehicle body, central body, rear body, front wheel & axle and rear wheel & axle, respectively. Coordinates x_7 and x_8 represent the rigid bases at the front and rear tires. Stiffness elements include body flexure, suspensions and tires; these are formulated using the Voight model (stiffness and damping elements in parallel), as shown in Fig. 1(a). Alternate engine mount sub-systems could then be incorporated into the vehicle model. These are summarized in Table 1 including: (i) rubber mount

described by the Voight model (resulting in a 6 DOF linear vehicle model), as shown in Fig. 1(b); (ii) quasi-linear hydraulic mount formulation [3] (leading to a 7 DOF quasi-linear vehicle model in Fig. 1(c)); and (iii) non-linear fluid or approximate mount formulations (yielding 8 DOF non-linear vehicle models), as shown by Figs. 1(d-e). Mathematical descriptions of such non-linear models will be given later in this paper.

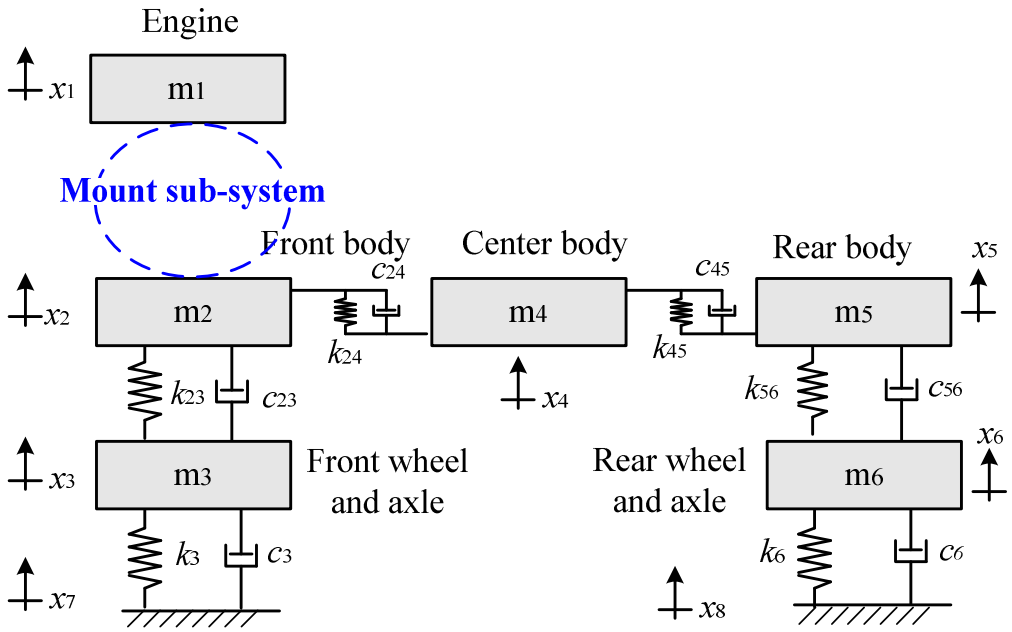

(a) 6 DOF half-vehicle model incorporating mount sub-system;

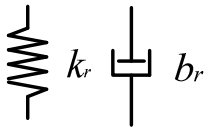

(b) rubber mount sub-system;

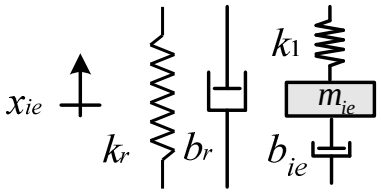

(c) quasi-linear hydraulic mount sub-system;

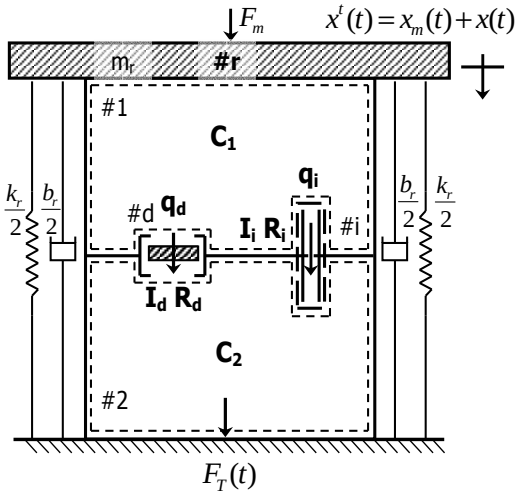

(d) fluid model of the non-linear hydraulic mount sub-system;

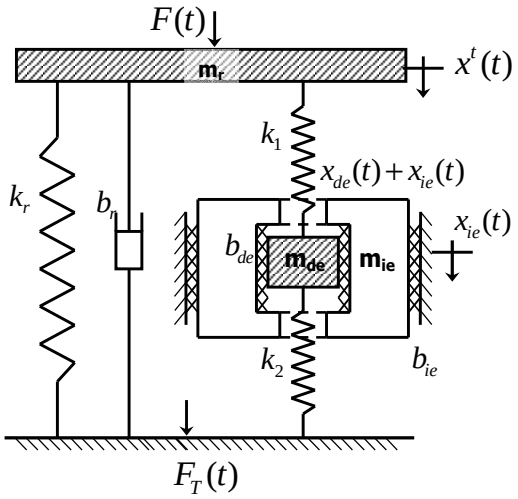

(e) approximate model of the non-linear hydraulic mount sub-system.

Fig. 1 Vehicle system and sub-system examples. Also, see Table 1.

MODAL ANALYSIS BASED ON QUASI-LINEAR MODEL

First, analytical modal analysis is conducted for the rubber mount of Fig. 1(b) as benchmark. Given nominal mass, stiffness and damping values of Table 2, the following six vehicle modes are obtained: (1) vehicle bounce; (2) engine bounce; (3) rear wheel hop; (4) front wheel hop; and (5) and (6) are vehicle body pitch and beaming (though the discrete model does not have enough resolution for these). The natural frequencies f_n and estimated modal damping ratios ζ are listed in Table 3. Here, we are most concerned about the engine bounce mode of Fig. 2, which shows some coupling with rear body and axle. Also, this mode is found to be most sensitive to the parameters of the mount sub-system.

Table 2 Parameters of half-vehicle model of Fig. 1(a)

Mass m (kg)	
m_1 (Powertrain)	125
m_2 (Front Body)	220
m_3 (Wheel+Axle)	45
m_4 (Center Body)	270
m_5 (Rear Body)	240
m_6 (Wheel+Axle)	75

Element	k (N/mm)		c (N-s/m)	
PT mount	k_r	300*	b_r	150*
Front suspension	k_{23}	22	c_{23}	200
Front tire	k_3	200	c_3	40
Body flexure	k_{24}	2,000	c_{24}	75
Body flexure	k_{45}	1,800	c_{45}	75
Rear suspension	k_{56}	26	c_{56}	200
Rear tire	k_6	200	c_6	40

*Baseline values for the rubber mount

Table 3 Vibration modes of 6 DOF half-vehicle model with rubber mount of Fig. 1(b)

Index	Mode Type	f_n (Hz)	ζ (%)
1	Vehicle bounce	1.1	2.6
2	**Engine bounce**	**8.0**	**1.1**
3	Rear wheel hop	8.7	3.0
4	Front wheel hop	11.2	3.8
5	Vehicle pitch	15.3	1.0
6	Body bending	24.1	0.5

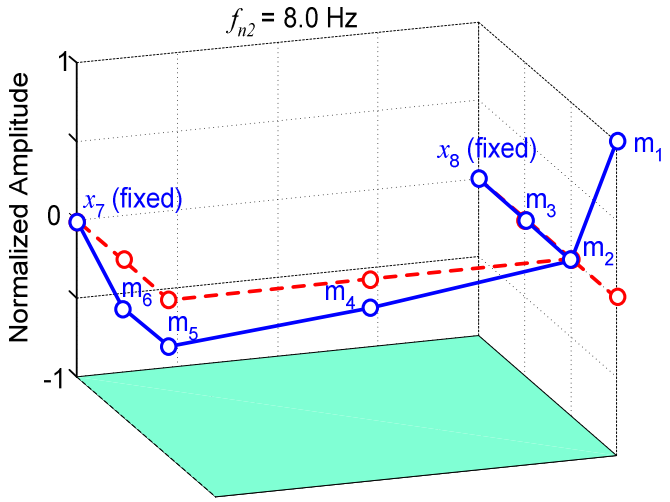

Fig. 2 Engine bounce mode with rubber mount sub-system.

Under certain operational conditions, the quasi-linear formulation [3] of Fig. 1(c) leads to a lumped parameter representation of the hydraulic mount sub-system in terms of equivalent spring, mass, damper elements. Thus, modal analysis and frequency response studies could be carried out in the context of vehicle dynamics. This should provide alternate and rapid evaluation of the tuning capability of hydraulic mount. An example case is provided here using the quasi-linear parameters estimated for one hydraulic mount (designated as D) at X = 2mm with k_1 = 344 N/mm, k_r = 379 N/mm, b_r = 142 Nm/s, b_{ie} = 2300 Nm/s and m_{ie} = 37.6 kg. Table 4 lists the resulting natural frequencies f_n and estimated modal damping ratios ζ. The engine bounce mode of Fig. 2 with rubber mount now seems to be transformed into two new coupled modes as shown in Fig. 3. The rest of vehicle modes remain almost unaffected.

Table 4 Modes of half-vehicle model with hydraulic mount described by a quasi-linear model of Fig 1(c)

Index	Mode Type	fn (Hz)	ζ (%)
1	Vehicle bounce	1.1	2.6
2	**Coupled mode I (in phase)**	**8.2**	**20.3**
3	Rear wheel hop	8.7	3.0
4	Front wheel hop	11.2	3.8
5	Vehicle pitch	15.6	21.5
6	**Coupled mode II (out of phase)**	**16.6**	**4.8**
7	Body bending	24.1	0.9

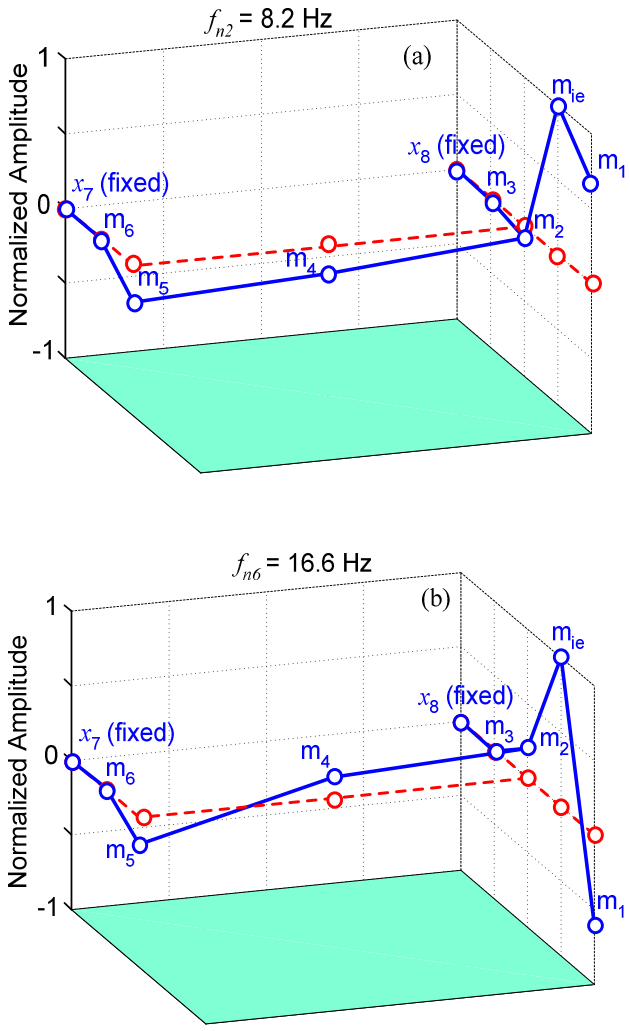

Fig. 3 Coupled engine bounce modes of half-vehicle model with hydraulic mount sub-system of Fig. 1(c) formulated using the quasi-linear model. (a) In-phase mode; (b) Out-of-phase mode.

Observe the following: First, m_{ie} and m_1 vibrate in phase for the mode depicted by Fig. 3(a), while m_{ie} and m_1 are out of phase for the other coupled mode of Fig. 3(b). Second, the maximum amplitudes of new modes correspond to the effective inertia track mass m_{ie} instead of the engine inertia m_1, so that the "inertia track resonance mode" is dominant over the "engine bounce mode" for both cases. Third, since inertia track is intentionally designed to provide high fluid damping, the "inertia track resonance mode" is associated with high viscous damping, as clearly shown by the high modal damping ratios for these two coupled modes. For this specific case, ζ increases 4 and 20 times for the two new engine bounce modes. This reveals the superiority of a hydraulic mount over the conventional rubber mount in controlling engine bounce resonances. By correlating the mechanical elements to fluid parameters [3], the quasi-linear model could be efficiently used by vehicle designers to quantify the mount specifications.

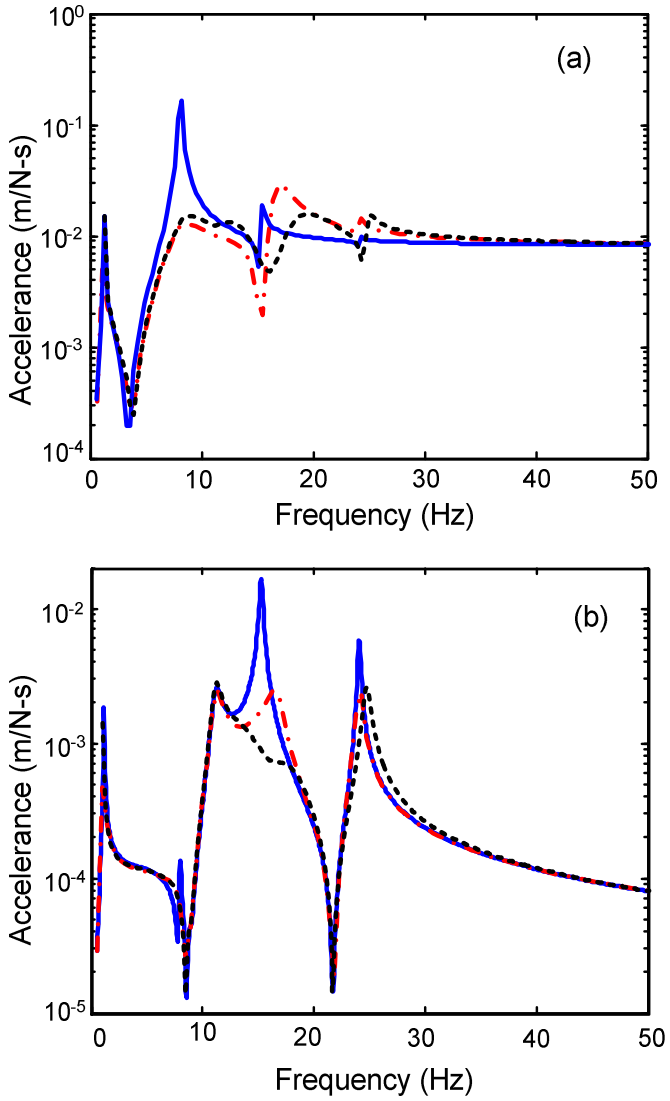

Fig. 4 Accelerance spectra (a) Accelerance A_1/F_1 at engine m_1 given force excitation from engine; (b) Accelerance A_2/F_3 at front body m_2 given force excitation from front wheel. Key: ——, rubber mount; – · – ·, hydraulic mount using quasi-linear formulation; – – – –, hydraulic mount using direct inversion method.

Next, frequency response functions (responses of displacement $X(f)$, velocity $V(f)$ or acceleration $A(f)$ given unit force excitation $F(f)$) are derived by using the quasi-linear formulation. These are then compared to those yielded by the direct inversion method given measured dynamic stiffness data (as benchmark) to quantify the errors induced by the quasi-linear estimation algorithm. Fig. 4(a) shows the A_1/F_1 engine accelerance given unit-amplitude engine force excitation. Likewise, Fig. 4(b) shows the A_2/F_3 front body accelerance given unit-amplitude front wheel force excitation. Compared with the rubber mount, the hydraulic mount sufficiently controls the engine bounce resonance around 8 Hz in Fig. 4(a), as well as the vehicle pitch resonance around 16 Hz in Fig. 4(b).

Comparison results of Fig. 4 imply that hydraulic mount can be utilized to provide not only high damping for engine motion control, but it also provides additional coupling between vehicle sub-systems. Such coupling could be useful in solving some vehicle vibration problems (such as the pitch resonance) that are encountered in sub-systems away from the engine mounts. Minor discrepancies exist between the quasi-linear model predictions and the direct inversion method due to the approximation process [3] and the assumption made in the process [3,8], i.e. $F_T(t) \approx F(t)$.

FLUID VS. APPROXIMATE NON-LINEAR MODELS OF HYDRAULIC MOUNTS

In a recent paper [3], we proposed a quasi-linear approximate model that utilizes steady state dynamic stiffness measurements to construct frequency- and excitation amplitude-sensitive mount models under certain operating conditions. Compared with a "true" non-linear fluid model, it significantly reduces the modeling effects and is capable of providing a quick assessment of the "augmented" damping and inertia effects [3,4]. Yet, the quasi-linear model is not sufficiently accurate to describe the non-linear responses especially for the decoupler mechanism. Therefore, an improved non-linear approximate model is developed as follows with an aim to capture the on-off switching actions of the decoupler. We will employ a clearance type element, while inheriting effective parameters from the quasi-linear model for reduced modeling efforts.

FLUID SYSTEM FORMULATION

The non-linear fluid model of Fig. 5 is briefly introduced here to derive the approximate model as well as for the sake of comparison. Refer to [5,6] for detailed description of the model and its experimental validation.

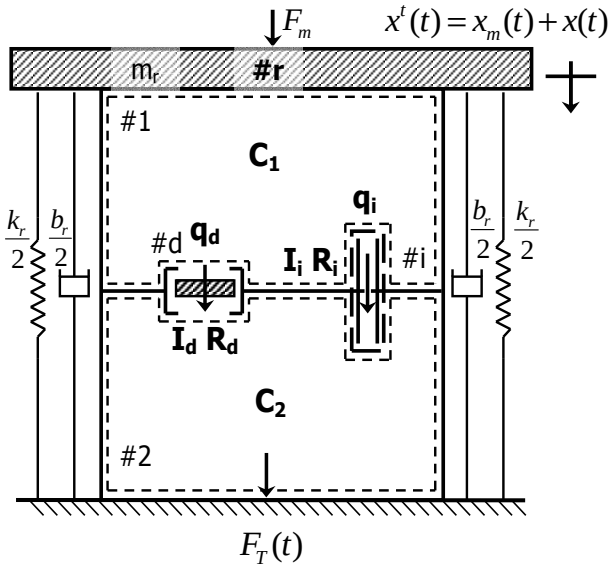

Fig. 5 Non-linear fluid model of the hydraulic mount with inertia track and decoupler.

The "virtual" driving point force $F(t)$ could be defined as follows where $x(t)$ is the piston displacement; m_r, b_r and k_r are the mass, damping and stiffness of rubber element; $p_1(t)$ is the dynamic pressure of the top chamber and A_r is the effective piston area.

$$F(t) = m_r\ddot{x}(t) + b_r\dot{x}(t) + k_r x(t) + A_r p_1(t) \quad (1)$$

Continuity equations for the top and bottom chambers yield:

$$A_r\dot{x}(t) - q_i(t) - q_d(t) = C_1(p_1)\dot{p}_1(t), \quad (2)$$

$$q_i(t) + q_d(t) = C_2(x_m)\dot{p}_2(t). \quad (3)$$

Here, $C_1(p_1)$ is the multi-staged top chamber compliance; $C_2(x_m)$ is the bottom chamber compliance sensitive to mean displacement x_m; $q_i(t)$ and $q_d(t)$ are the volumetric flow rates through the inertia track (i) and decoupler (d), respectively. Momentum equations for the decoupler and inertia track yield the following, where I_d and I_i are the inertia of fluid columns; $R_i(q_i)$ and $R_d(q_d)$ are the non-linear resistances:

$$p_1(t) - p_2(t) = I_d\dot{q}_d(t) + R_d(q_d)q_d(t), \quad (4)$$

$$p_1(t) - p_2(t) = I_i\dot{q}_i(t) + R_i(q_i)q_i(t) \quad (5)$$

Note that Eq. (4) dictates the "decoupled" state when the decoupler gap is open, and Eq. (5) is dominant over the "coupled" state with the decoupler gap closes. The dynamic component of force $F_T(t)$ transmitted to the rigid base is derived and is related to $F(t)$ as follows:

$$F_T(t) = k_r x(t) + b_r\dot{x}(t) + A_r p_1(t) = F(t) - m_r\ddot{x}(t) \quad (6)$$

NON-LINEAR APPROXIMATE METHOD

An approximate mechanical model of Fig. 6 is developed for improved understanding of the decoupling effects of a free decoupler mount.

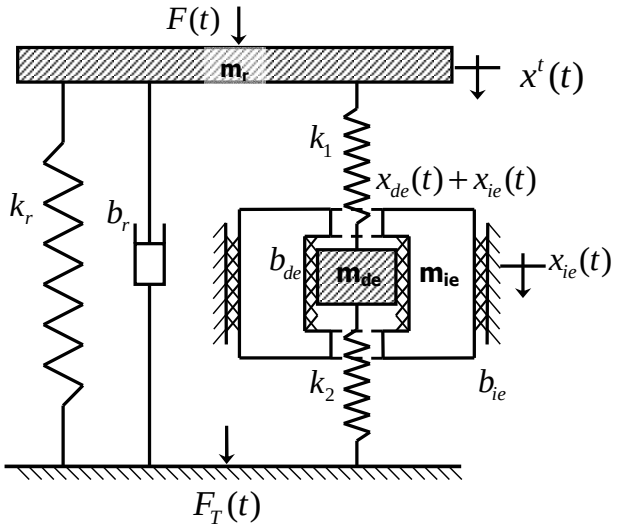

Fig. 6 Non-linear approximate model of the hydraulic mount with inertia track and decoupler

Note that all non-linear parameters such as $C_1(p_1)$ are modeled as a function of the nominal excitation amplitude X. The switching mechanism is described in terms of a clearance type non-linearity and the effective parameters as described in [3] could be directly incorporated into the approximate model. Given equations (1-6) and parameters of Table 5, the non-linear approximate model of Fig. 6 is derived as follows, where $x_{ie}(t)$ is the (absolute) displacement of the inertia track fluid mass m_{ie}, and $x_{de}(t)$ is the relative displacement between the effective masses m_{de} and m_{ie}. The absolute displacement of m_{de} is therefore $x_{ie}(t) + x_{de}(t)$.

Table 5 Physical and effective parameters of the approximate model of Fig. 6

Parameters	Physical value	Effective value
Inertia track fluid mass	$m_i = A_i^2 I_i$	$m_{ie} = A_r^2 I_i$
Decoupler mass	$m_d = A_d^2 I_d$	$m_{de} = A_r^2 I_d$
Inertia track damping	$b_i = A_i^2 R_i$	$b_{ie} = A_r^2 R_i$
Decoupler damping	$b_d = A_d^2 R_d$	$b_{de} = A_r^2 R_d$
Inertia track displacement	$x_i(t) = \frac{\int q_i(t)dt}{A_i}$	$x_{ie}(t) = \frac{\int q_i(t)dt}{A_r}$
Decoupler displacement	$x_d(t) = \frac{\int q_d(t)dt}{A_d}$	$x_{de}(t) = \frac{\int q_d(t)dt}{A_r}$
Decoupler gap length	l_g	$l_{ge} = l_g \frac{A_d}{A_r}$
Top chamber fluid stiffness	---	$k_1 = A_r^2 / C_1$
Bottom chamber fluid stiffness	---	$k_2 = A_r^2 / C_2$

The effective (but virtual) dynamic force at the driving point of Fig. 6 is derived as:

$$F(t) = m_r \ddot{x}(t) + k_r x(t) + b_r \dot{x}(t) + k_1\left[x(t) - x_{ie}(t) - x_{de}(t)\right] \quad (7)$$

In the "decoupled" state, the decoupler gap is open such that $0 < x_{de}(t) < l_{ge}$. Fluid flows mainly through the decoupler gap since $R_i >> R_d$ (or $b_{ie} >> b_{de}$). Consequently, $q_i(t) << q_d(t)$, or $\dot{x}_{ie}(t) << \dot{x}_{de}(t)$ and $\ddot{x}_{ie}(t) << \ddot{x}_{de}(t)$.

Fluid equations (2-4) are rewritten in terms of the mechanical system symbols of Table 5 as follows:

$$m_{de}\ddot{x}_{de}(t) + b_{de}\dot{x}_{de}(t) + k_1\left[x_{ie}(t) + x_{de}(t) - x(t)\right] + k_2\left[x_{ie}(t) + x_{de}(t)\right] = 0,$$

"decoupled" state ($0 < x_{de}(t) < l_{ge}$) (8a)

Since $\ddot{x}_{de}(t) \approx \ddot{x}_{de}(t) + \ddot{x}_{ie}(t)$, Eq. (8a) is approximated by Eq. (8b), which dictates the dynamics of m_{de} during the "decoupled" state, when a relative motion $\dot{x}_{de}(t)$ exists between m_{de} and m_{ie}.

$$m_{de}\left[\ddot{x}_{de}(t) + \ddot{x}_{ie}(t)\right] + b_{de}\dot{x}_{de}(t) + k_2[x_{ie}(t) + x_{de}(t)] + k_1[x_{ie}(t) + x_{de}(t) - x(t)] = 0,$$

"decoupled" state ($0 < x_{de}(t) < l_{ge}$) (8b)

Eqs. (4-5) also lead to the system equation as follows:

$$m_{ie}\ddot{x}_{ie}(t) + b_{ie}\dot{x}_{ie}(t) = m_{de}\ddot{x}_{de}(t) + b_{de}\dot{x}_{de}(t),$$

"decoupled" state ($0 < x_{de}(t) < l_{ge}$) (9a)

Over the lower frequency range, say up to 50 Hz, assume that the decoupler viscous force is dominant so that $b_{de}\dot{x}_{de}(t) >> m_{de}\ddot{x}_{de}(t)$. Eq. (9a) is then approximated by Eq. (9b) corresponding to the governing equation of m_{ie} during the "decoupled" state.

$$m_{ie}\ddot{x}_{ie}(t) + b_{ie}\dot{x}_{ie}(t) - b_{de}\dot{x}_{de}(t) = 0,$$

"decoupled" state ($0 < x_{de}(t) < l_{ge}$) (9b)

During the "coupled" state, the decoupler gap is closed so that $x_{de} = 0$ or $x_{de} = l_{ge}$. No fluid flows through the decoupler gap, i.e. $q_d(t) = 0$ or $\dot{x}_{de} = 0$ and $\ddot{x}_{de} = 0$. This implies no relative motion exists between m_{de} and m_{ie}. Eqs (2, 3, 5) are converted into:

$$m_{ie}\ddot{x}_{ie}(t) + b_{ie}\dot{x}_{ie}(t) + k_1[x_{ie}(t) - x(t)] + k_2 x_{ie}(t) = 0,$$

"coupled" state ($x_{de} = 0$ or l_{ge}) (10a)

Since $m_{ie} >> m_{de}$, Eq. (10a) is approximated by Eq. (10b), which dictates the dynamic motion of combined masses $m_{ie} + m_{de}$ while moving together after reaching either the top or bottom stop.

$$\left(m_{ie} + m_{de}\right)\ddot{x}_{ie}(t) + b_{ie}\dot{x}_{ie}(t) + k_1[x_{ie}(t) - x(t)] + k_2 x_{ie}(t) = 0,$$

"coupled" state ($x_{de} = 0$ or l_{ge}) (10b)

Finally, for both states, $F_T(t)$ is converted from Eq. (6) to the following:

$$F_T(t) = k_r x(t) + b_r \dot{x}(t) + k_1\left[x(t) - x_{ie}(t) - x_{de}(t)\right] \quad (11)$$

The switching mechanism between the "decoupled" and "coupled" states is converted into a clearance type non-linearity in the approximate model of Fig. 6: When the excitation amplitude of $x(t)$ is small enough so that m_{de} travels without reaching the top or bottom stop ($0 < x_{de}(t) < l_{ge}$), m_{ie} is decoupled from the mount system. Thus the system is in a "soft" state dictated by Eqs. (8b) and (9b) yielding reduced stiffness and damping. Under higher excitation amplitudes, when m_{de} reaches the top or bottom stop (x_{de} = 0 or l_{ge}), m_{ie} moves along with m_{de} and the system is described by Eq. (10b). The inertia track is thus "coupled" into the system providing high fluid resistance b_{ie}. Note that our quasi-linear model [3] is essentially a limiting case of this when b_{de} (or R_d) approaches infinity. The compressive contact force $F_c(t)$ between m_{de} and m_{ie} is formulated as:

$$F_c(t) = \begin{cases} m_{de}\ddot{x}_{ie}(t) + F_2(t) - F_1(t), & x_{de} = l_{ge} \\ -m_{de}\ddot{x}_{ie}(t) - F_2(t) + F_1(t), & x_{de} = 0 \end{cases} \quad \text{(12a)}$$

where $F_1(t) = k_1\left[x(t) - x_{ie}(t)\right]$ and $F_2(t) = k_2 x_{ie}(t)$ are the effective "elastic" forces analogous to the top and bottom chamber pressure forces $p_1(t)A_r$ and $p_2(t)A_r$. Since the decoupler is typically designed like a flow control valve, its inertial force $m_{de}\ddot{x}_{ie}(t)$ is negligible compared with the "elastic" force. Hence, the switching condition from the "coupled" to the "decoupled" state is converted from Eq. (12a) to the following:

$$\begin{cases} F_2(t) - F_1(t) < 0, & x_{de} = l_{ge} \\ F_2(t) - F_1(t) > 0, & x_{de} = 0 \end{cases} \quad \text{(12b)}$$

COMPARISON BETWEEN TWO NONLINEAR MODELS

The non-linear approximate model is next compared with a validated non-linear fluid model [5,6] in both time and frequency domains. Assuming a sinusoidal displacement x(t) with f = 5 Hz and X = 1 mm (p-p), Fig. 7(a) depicts the dynamic chamber pressures $p_1(t)$ and $p_2(t)$ that are predicted by the fluid model. And, Fig. 7(b) shows the contact force $F_1(t)$ and $F_2(t)$ waveforms as predicted by the approximate model. Observe that predicted waveforms share essentially the same characteristics. The spikes in $p_1(t)$ or $F_1(t)$ correspond to the time instants when the decoupler is closed in the fluid system or when m_{ie} is "coupled" with m_{de} in the approximate system; the flat regions in $p_1(t)$ or $F_1(t)$ are associated with the operation conditions such that the decoupler is open or when m_{de} loses contact with m_{ie} in the "decoupled" state. The $p_2(t)$ and $F_2(t)$ waveforms are comparatively smoother due to the fact that C_2 >> C1 in the fluid system, or k_1 >> k_2 in the approximate model.

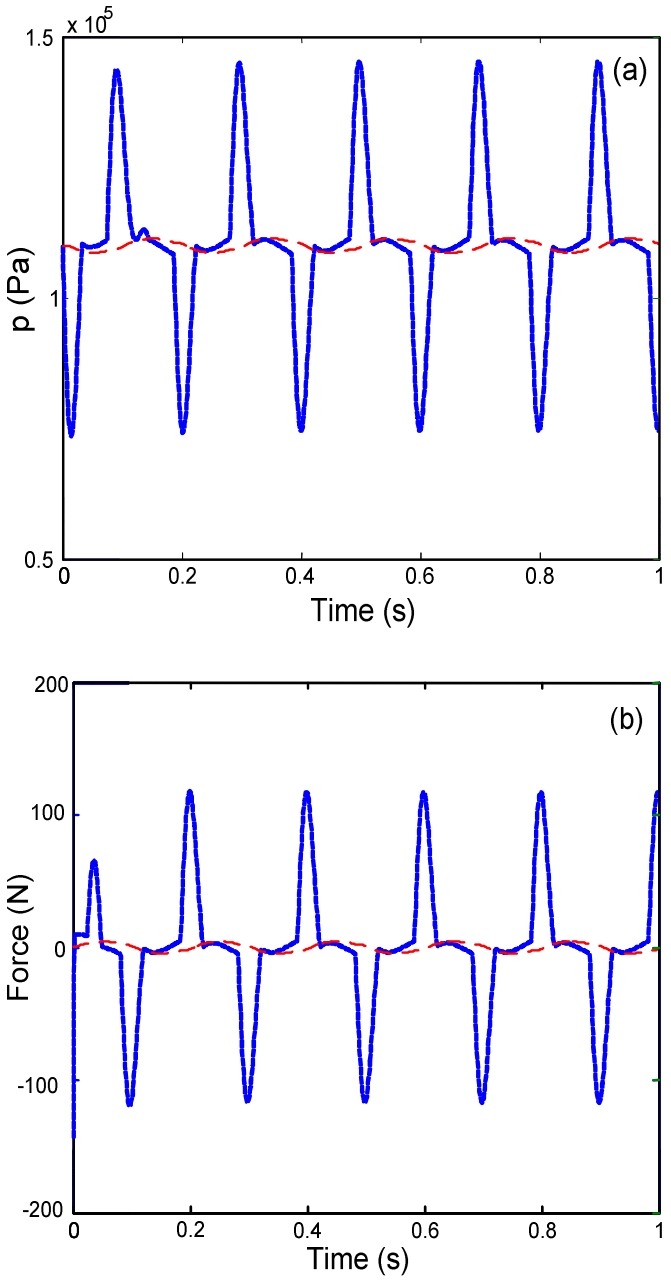

Fig. 7 Dynamic responses given sinusoidal displacement excitation with X = 1.0 mm and f = 5 Hz: (a) $p_1(t)$ and $p_2(t)$ predicted by the fluid model; (b) elastic contact forces $F_1(t)$ and $F_2(t)$ predicted by the approximate model. Key: ——, $p_1(t)$ or $F_1(t)$; – – –, $p_2(t)$ or $F_2(t)$.

In Fig. 8, simulated dynamic stiffness data are compared. They are from the fluid and approximate models under harmonic excitations with amplitudes ranging from 0.3 to 3 mm (p-p) in up to 50 Hz. Nearly identical dynamic stiffness spectra are obtained, which confirms that the approximate model with clearance non-linearity indeed captures the decoupler switching mechanism of the fluid model in Fig. 5.

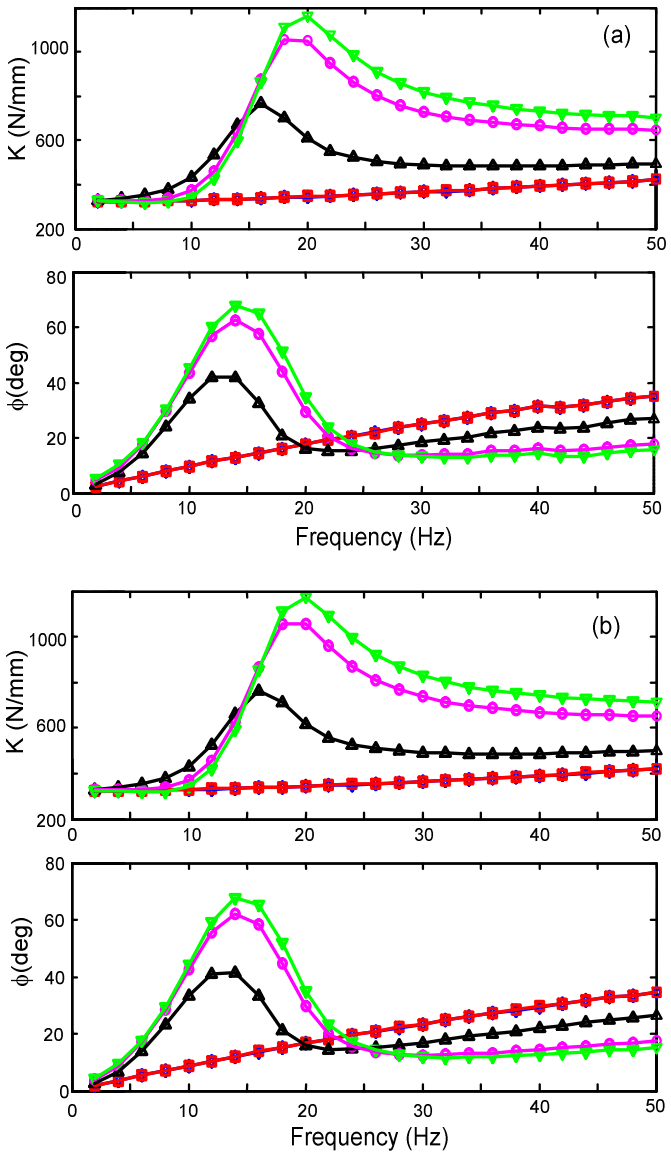

Fig. 8 Dynamic stiffness predicted using (a) fluid model with free decoupler; (b) approximate model with clearance non-linearity. Key: ◊, X = 0.3 mm (p-p); □, X = 0.5 mm (p-p); △, X = 1 mm (p-p); ○, X = 2 mm (p-p); ▽, X = 3 mm (p-p).

INCOPORATION OF NON-LINEAR MODELS INTO VEHICLE SYSTEM

Next, non-linear hydraulic mount models are incorporated into the vehicle system and compared with linear and quasi-linear formulations. Key governing equations of the non-linear vehicle system with fluid type mount are given as follows; comparable vehicle formulations including the non-linear approximate mount could also be derived by combining Eqs. (8) to (12) with other vehicle components in a similar manner. With reference to Figs. 1(a) and 1(d), where the positive directions of $x_i(t)$ are taken to be upward, the engine dynamics is described as:

$$\begin{aligned}&(m_r+m_1)\ddot{x}_1(t)+b_r\left[\dot{x}_1(t)-\dot{x}_2(t)\right]+k_r\left[x_1(t)-x_2(t)\right]\\&-A_r p_1(t)=|F_e|\sin\left(2\pi f_e t+\phi_e\right)\end{aligned} \quad (13)$$

The continuity equation for the bottom chamber remains the same as Eq. (3), and the continuity equation for the top chamber now changes to:

$$A_r\left[\dot{x}_1(t)-\dot{x}_2(t)\right]-q_i(t)-q_d(t)=C_1(p_1)\dot{p}_1(t) \quad (14)$$

Governing equations for the decoupler and inertia track dynamics remain the same as Eqs. (4) and (5), respectively, while the transmitted force is now:

$$F_T(t)=k_r\left[x_2(t)-x_1(t)\right]+b_r\left[\dot{x}_2(t)-\dot{x}_1(t)\right]+A_r p_1(t) \quad (15)$$

Dynamics of the front body is dictated by:

$$\begin{aligned}&m_2\ddot{x}_2(t)+k_r\left[x_2(t)-x_1(t)\right]+b_r\left[\dot{x}_2(t)-\dot{x}_1(t)\right]\\&+A_r p_1(t)+k_{23}\left[x_2(t)-x_3(t)\right]+k_{24}\left[x_2(t)-x_4(t)\right]\\&+c_{23}\left[\dot{x}_2(t)-\dot{x}_3(t)\right]+c_{24}\left[\dot{x}_2(t)-\dot{x}_4(t)\right]=0\end{aligned} \quad (16)$$

The rest of the governing equations not directly involved with the hydraulic mount sub-system could be easily derived.

Vehicle responses are calculated in both time and frequency domains given engine force excitations. Since higher harmonics are not easily distinguished from the time domain responses, only the frequency spectra are presented here in order to compare linear and quasi-linear vehicle models. Figs. 9-10 compare results of vehicle mass displacements or accelerations given sinusoidal engine force with the amplitude of 1000 N at 10 Hz. In Fig. 9, the engine response is shown to be most sensitive to the mounting system, and the engine bounce resonance at 8.4 Hz (with rubber mount) is reduced up to 40 dB by using the hydraulic mount. The vehicle pitch resonance around 15 Hz is also affected due to a coupling between hydraulic mount and other vehicle components.

Given the same sinusoidal excitation with amplitude of 1000 N at 10 Hz, Fig. 10 compares the dynamic vehicle accelerations predicted by using the quasi-linear formulation and by using the non-linear fluid model (with fixed decoupler), respectively. Observe that: (i) The slopes of the acceleration spectra predicted by both models match well with each other. (ii) Both models capture the basic vehicle resonances which were predicted by the modal analysis. Recall Table 4 for the natural frequencies and estimated modal damping ratios corresponding to these resonances. (iii) The wheel hop resonance around 11 Hz is dominating the dynamic responses, and its super-harmonics at the multiples of the fundamental frequency are predicted only by the non-linear fluid (or approximate) model. This confirms the necessity of incorporating non-linear hydraulic mount formulation into the vehicle system for examining non-linear phenomena such as the super-harmonics.

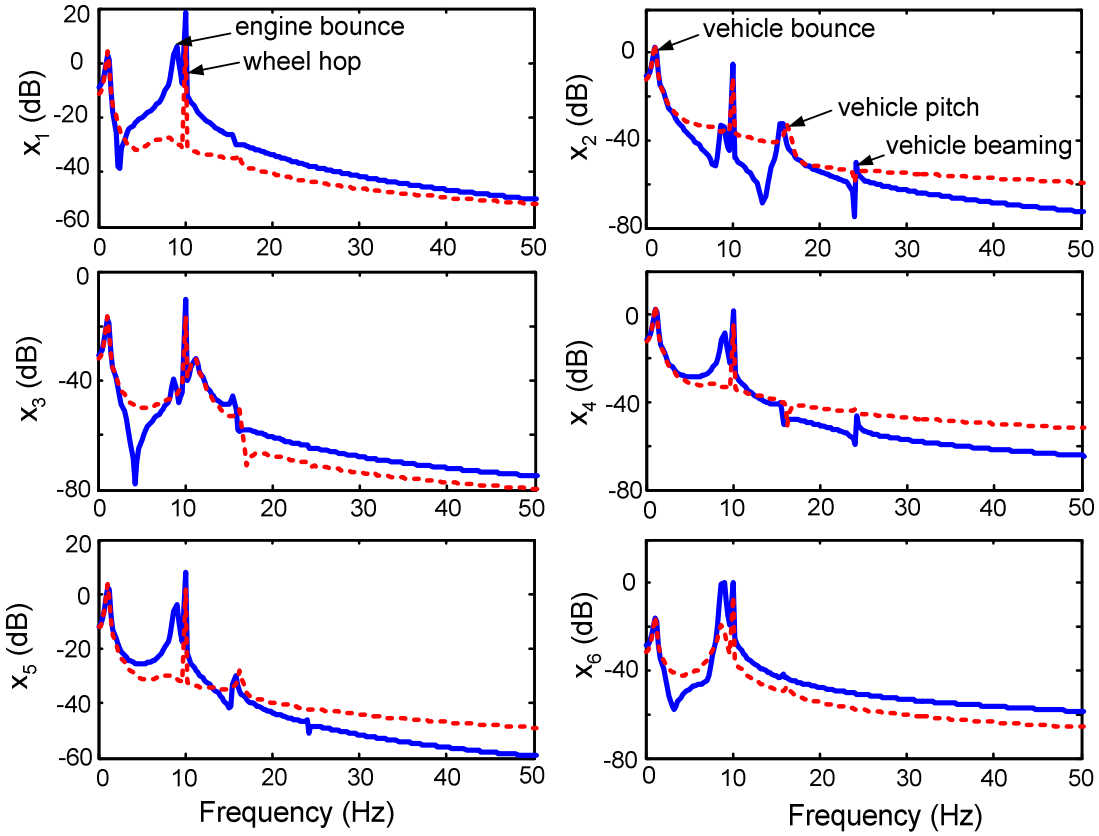

Fig. 9 Predicted vehicle displacement spectra (dB re 1 mm) given sinusoidal engine force excitation with an amplitude of 1000 N at 10 Hz. Key: ——, linear model with rubber mount; – – –, quasi-linear model with hydraulic mount.

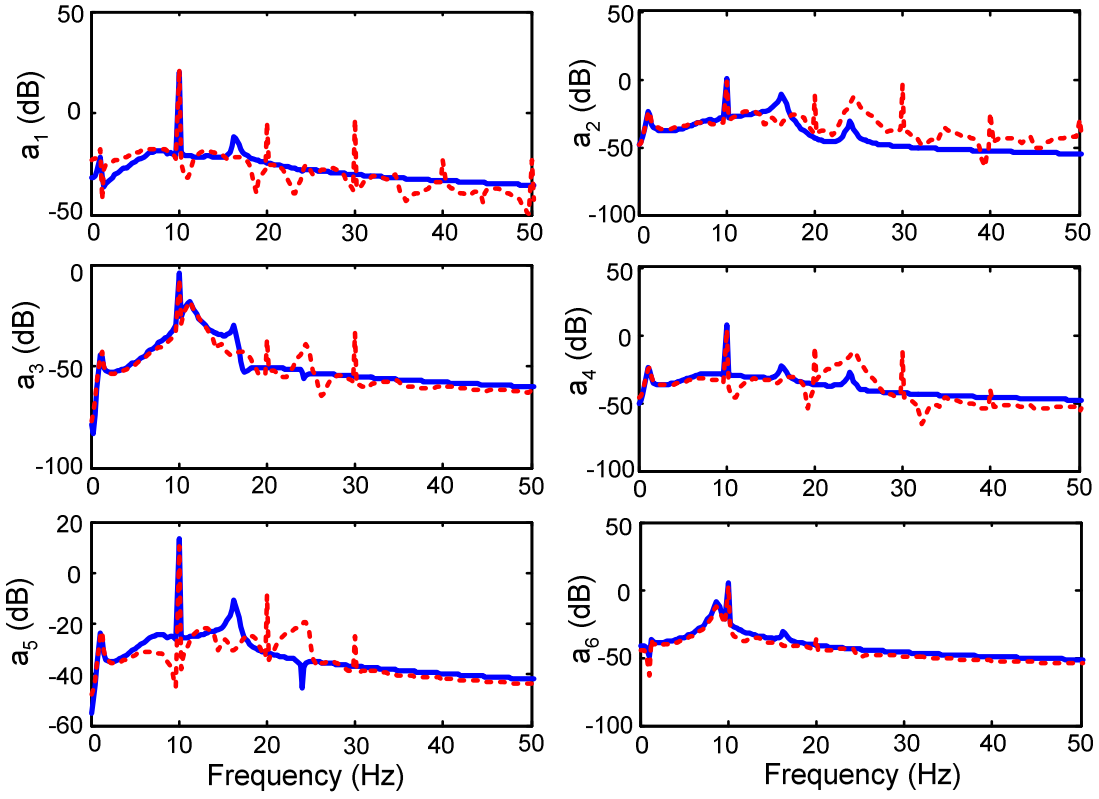

Fig. 10 Predicted vehicle acceleration spectra (dB re 1 m/s^2) given sinusoidal engine force excitation with an amplitude of 1000 N at 10 Hz. Key: ——, quasi-linear model with hydraulic mount; – – –, non-linear fluid model with fixed decoupler.

CONCLUSION

This paper has comparatively evaluated linear, quasi-linear and "true" non-linear (approximate and fluid type) models of hydraulic engine mounts and examined their dynamic effects in a simplified half-vehicle system. A non-linear approximate model is developed to provide improved insight into the decoupling effects. Hydraulic mount is shown to be highly efficient in providing high damping and in tuning vehicle dynamics. Proposed vehicle models could be effectively utilized to examine vehicle responses in both time and frequency domains. Our vehicle models (in alternate forms) could serve as the platform for further research into improved estimations of damping and stiffness models, better predictions in time domain as well as refinements of the vehicle design and integrations issues. The fundamental question of "importing" measured data (given displacement excitation and blocked boundary in the elastomer test method) and incorporating them in a system with realistic boundaries and force excitations is yet to be resolved. We are examining this issue and will provide some guidance in future papers.

ACKNOWLEDGMENTS

We acknowledge the experimental efforts of M. Tiwari and J. Sorenson from 1999 to 2002. Those studies were financially supported by the Ford Motor Company. We thank Dr. J. H. Lee for his comments and suggestions.

REFERENCES

1. R. Singh, G. Kim and P. V. Ravindra, "Linear analysis of automotive hydro-mechanical mount with emphasis on decoupler characteristics", J. Sound Vib. 158, 219-243 (1992).
2. G. Kim and R. Singh, "Study of Passive and Adaptive Hydraulic Engine Mount Systems with Emphasis on Nonlinear Characteristics", J. Sound Vib. 179, 427-453 (1995).
3. S. He and R. Singh, "Estimation of Amplitude and Frequency Dependent Parameters of Hydraulic Engine Mount Given Limited Dynamic Stiffness Measurements", Noise Control Eng. J., 53(6), 271-285, (2005).
4. J. E. Colgate, C. T. Chang, Y. C. Chiou, W. K. Liu and L. M. Keer, "Modeling of a Hydraulic Engine Mount Focusing on Response to Sinusoidal and Composite Excitations", J. Sound Vib., 184(3), 503-528 (1995).
5. M. Tiwari, H. Adiguna and R. Singh, "Experimental Characterization of a Nonlinear Hydraulic Engine Mount", Noise Control Eng. J. 51(1), 36-49 (2003).
6. H. Adiguna, M. Tiwari and R. Singh, "Transient Response of a Hydraulic Engine Mount", J. Sound Vib. 268, 217-248 (2003).
7. Y. Yu, N. G. Naganathan and R. V. Dukkipati, "A Literature Review of Automotive Vehicle Engine Mounting Systems", J. Dynamic Sys, Measurement, and Control, 123(2), 186-194 (2001).
8. J. H. Lee, M. S. Bae and K. J. Kim, "Limitations of Mechanical Model With Lumped Mass in Representing Dynamic Characteristics of Hydraulic Mount", SAE Paper 2003-01-1466 (2003).
9. N. Tsujiuchi, T. Koizumi and K. Yamazaki. "Vibration Analysis of Engine Supported by Hydraulic Mounts", SAE Paper 2003-01-1465 (2003).
10. T. Jeong and R. Singh, "Inclusion of Measured Frequency-and Amplitude-Dependent Mount Properties in Vehicle or Machinery Models", J. Sound Vib. 245, 385-415 (2001).
11. S. B. Choi and H. J. Song, "Vibration Control of a Passenger Vehicle Utilizing a Semi-Active ER Engine Mount", J. Vehicle Sys. Dynamics, 37(3), 193-216, (2002).

CONTACT

Professor Rajendra Singh
Acoustics and Dynamics Laboratory
Center for Automotive Research and
NSF I/UCRC Smart Vehicle Concepts Center
The Ohio State University
Email: singh.3@osu.edu
Phone: 614-292-9044
Website: www.AutoNVH.org